Enclosure
Relief Request 52 Proposed Alternative in Accordance with 10 CFR 50.55a(a)(3)(i)

ATTACHMENT 5

Palo Verde Unit 3 - BMI Nozzle Crack Growth Analysis

AREVA

CALCULATION SUMMARY SHEET (CSS)

Document No. 32 - 9222043 - 000 Safety Related: ☒Yes ☐ No

Title Palo Verde Unit 3 - BMI Nozzle Crack Growth Analysis (Non-Proprietary)

PURPOSE AND SUMMARY OF RESULTS:

The purpose of this calculation is to perform a conservative crack growth analysis to demonstrate that radial axial flaws in the BMI nozzle No. 3 will not grow large enough to reach both ends of the nozzle, before the plant license expiration in 2047. Both primary water stress corrosion cracking (PWSCC) and fatigue crack growth (FCG) mechanisms will be considered.

Based on NDE, an initial surface crack with depth, a= [ ], and length, 2c= [ ] was postulated. This crack will grow to be through wall in [ ] years at which time it will have a length, 2c= [ ].

In an additional [ ] years, the crack length will grow to 2c= [ ], at which time it will grow to the end of the bottom portion of the nozzle, which is confined below the j-groove weld and the reactor vessel bore and as such will not become a loose part.

In the remaining [ ] years until plant license expiration in 2047 the crack grows up the nozzle to a total length of approximately a= [ ]; this leaves a remaining un-cracked ligament of approximately [ ] inches at the top of the nozzle so the generation of loose parts is unlikely.

This is the Non-Proprietary version of 32-9217241-002.

AREVA Inc. proprietary information in the document is indicated by pairs of brackets "[ ]".

THE FOLLOWING COMPUTER CODES HAVE BEEN USED IN THIS DOCUMENT:		THE DOCUMENT CONTAINS ASSUMPTIONS THAT SHALL BE VERIFIED PRIOR TO USE
CODE/VERSION/REV	CODE/VERSION/REV	☐Yes
None		☒ No

Review Method: ☒ Design Review (Detailed Check)

☐ Alternate Calculation

Signature Block

Name and Title (printed or typed)	Signature	P/R/A and LP/LR	Date	Pages/Sections Prepared/Reviewed/Approved
Tom Riordan Engineer III		P	18APR2014	All
Doug Killian, Technical Consultant		R	4/18/14	All
Tim Wiger, Unit Manager		A	4/18/14	All

Note: P/R/A designates Preparer (P), Reviewer (R), Approver (A);
LP/LR designates Lead Preparer (LP), Lead Reviewer (LR)

Project Manager Approval of Customer References (N/A if not applicable)

Name (printed or typed)	Title (printed or typed)	Signature	Date
Maya Chandrashekhar	Project Manager		4/18/14

Mentoring Information (not required per 0402-01)

Name (printed or typed)	Title (printed or typed)	Mentor to: (P/R)	Signature	Date
N/A				

Record of Revision

Revision No.	Pages/Sections/Paragraphs Changed	Brief Description / Change Authorization
000	All	Initial Release

Table of Contents

Page

SIGNATURE BLOCK 2

RECORD OF REVISION 3

LIST OF TABLES 5

LIST OF FIGURES 6

1.0 INTRODUCTION 7

2.0 ANALYTICAL METHODOLOGY 7

3.0 ASSUMPTIONS 10

4.0 ANALYSIS INPUTS 11
- 4.1 Geometry and Material 11
- 4.2 Bounding Initial Flaw Size 11
- 4.3 Loading Data and Stresses 12

5.0 CALCULATIONS 13
- 5.1 Path Lines for Stresses 13
- 5.2 Growth of Initial Surface Crack 13
- 5.3 Growth of Through Wall Crack 15
- 5.4 Growth of Single Edge Notched Plate Crack 19
- 5.5 Stability Check 26

6.0 SUMMARY OF RESULTS 27

7.0 REFERENCES 28

APPENDIX A : BOUNDING AXIAL FLAW IN NOZZLE A-1

APPENDIX B : COMPUTER FILES B-1

List of Tables

Page

Table 5-1: Crack Growth Calculation for Longitudinal Surface Flaw 14
Table 5-2: Crack Growth Calculation for Longitudinal Through Wall Flaw 15
Table 5-3: Crack Growth Calculation for Single Edge Notched Plate 20

Table A-1: UT Data for Flaw Indications 1 Through 4 ..... A-3
Table A-2: UT Data for Flaw Indications 5 Through 10 ..... A-4
Table A-3: Calculation of Nozzle Cutout A-5
Table B-1: List of Revision 000 Computer Files B-2
Table B-2: List of Revision 001 Computer Files B-5

List of Figures

Page

Figure 5-1: Path Lines for Stresses 13
Figure 6-1: Sketch of Flaw Growth Progression 27

Figure A-1: Reference Positions for UT Inspection Data A-2

1.0 INTRODUCTION

Non-destructive examination (NDE) of bottom mounted instrumentation (BMI) nozzle 3 at Palo Verde Unit 3 indicated the presence of ten predominantly axial cracks in the outer portion of the nozzle at the partial penetration weld to the vessel head. Although a half-nozzle repair performed on nozzle 3 moved the primary pressure boundary from the original J-groove partial penetration weld at the inner surface of the vessel to a new J-groove partial penetration weld at an outer surface weld pad, there remains a concern that cracks in the nozzle may propagate over the remaining life of the plant to the extent that loose parts are formed. AREVA Document 51-9220420 (latest revision) provides a road map of the AREVA analyses for the Palo Verde BMI Nozzle.

The purpose of this calculation is to perform a conservative crack growth analysis to demonstrate that radial axial flaws in the BMI nozzle No. 3 will not grow large enough to reach both ends of the nozzle, before the plant license expiration in 2047. Both primary water stress corrosion cracking (PWSCC) and fatigue crack growth (FCG) mechanisms will be considered.

2.0 ANALYTICAL METHODOLOGY

1. Based on NDE data, postulate a single bounding surface crack in the longitudinal (axial) direction, [ ] in depth by [ ] in length, on the outside of the nozzle near the uphill side of the original J-groove weld. See Appendix A for discussion of the NDE data and determination of the bounding axial flaw size. Assume the crack is centered at the location of maximum operating plus weld residual stress.

2. The stress intensity factor, K_I, for the surface crack is calculated using the solution from Section C.5.11 (Equation C.192) of API-579-1[1]. This is the solution for a cylinder, with a surface crack, in the longitudinal direction, an elliptical shape, and a through-wall fourth order polynomial stress distribution (API-579-1 Solution KCSCLE2). This solution is valid for crack depths up to 80% of the wall thickness.
   Equation C.192 of API-579-1 is:

$$K_I = \left[G_0\{\sigma_o + p_c\} + G_1\sigma_1\left(\frac{a}{t}\right) + G_2\sigma_2\left(\frac{a}{t}\right)^2 + G_3\sigma_3\left(\frac{a}{t}\right)^3 + G_4\sigma_4\left(\frac{a}{t}\right)^4 \right]\sqrt{\frac{\pi a}{Q}}$$

   Note that the influence coefficients, G_i, vary with elliptical angle φ, with $\varphi=0$ at the surface and $\varphi=\pi/2$ at the deepest point of the crack.

3. The stress intensity factor, K_I, for the through wall crack is calculated using the solution from Section C.5.1 (Equation C.156) of API-579-1. This is the solution for a long cylinder, with a through wall longitudinal crack and through-wall membrane and bending stress distributions (API Solution KCTCL).
   Equation C.156 of API-579-1 is:

$$K_I = \left[\{\sigma_m + p_c\}G_0 + \sigma_b(G_0 - 2G_1)\right]\sqrt{\pi c}$$

   As noted, the above solution is for a long cylinder; as the crack grows towards the end of the nozzle boundary effects can become important. To account for boundary effects correction factors are applied. The correction factor utilized is based on a polynomial fit to the data in Table 2.1 of Reference [2]. The resulting correction factor is

$$[\qquad\qquad]$$

   where 2c is the crack length and [ ] inches is the effective width of the plate (twice the distance from the crack centerline to the bottom of the nozzle).

4. If the through wall crack grows to 2c= [ ] the crack has essentially grown through the bottom of the remnant nozzle. At this point the stress intensity factor solution utilized is that for a single edge crack plate. From Reference [2] the solution is

$$K_I = \sigma\sqrt{\pi a} f\left(\frac{a}{b}\right)$$

where σ is the applied stress, a is the crack width, $2b$ is the plate width, and $f(a/b)$ is a correction factor given in Table 2.2 of Reference [2]. Conservatively, the applied stress utilized is the sum of the membrane stress, bending stress, and crack face pressure. The polynomial fit to the tabulated correction factor data is given below.

$$f\left(\frac{a}{b}\right) = 2.0492\left(\frac{a}{b}\right)^2 - 0.4245\left(\frac{a}{b}\right) + 1.1995$$

5. Stresses are obtained from References [3] and [4]. Hoop stresses are obtained at a set of through-wall pathlines closely spaced in the longitudinal direction.

   a. For the surface crack, the stress intensity solution requires that stresses be fit with a fourth-order polynomial:

$$\sigma(x) = \sigma_0 + \sigma_1\left(\frac{x}{t}\right) + \sigma_2\left(\frac{x}{t}\right)^2 + \sigma_3\left(\frac{x}{t}\right)^3 + +\sigma_4\left(\frac{x}{t}\right)^4$$

   For this purpose a single conservative pathline (within the region of the surface crack) is chosen and stresses are fit by least squares.

   b. For the through wall crack, the stress intensity solution requires membrane stress which is assumed constant. In reality, the membrane stress (through wall average hoop stress) varies over the width of the crack (axial location on the nozzle). The membrane and bending (through wall hoop) stress will be evaluated at a number of different axial positions on the nozzle. For evaluating crack growth rate, the average membrane and bending stress within the current crack length will be used.

   c. For the single edge notch plate the stress utilized will also be the average of the stresses over the current crack length.

6. Calculate the flaw growth versus time as follows:

   a. The surface crack starts with the length to depth ratio (aspect ratio) for the bounding crack defined in step 1. Growth in depth and length will be separately calculated for each time step by calculating the applied K_I at the surface and at the deepest part of the crack.

   b. The surface flaw is grown until it propagates to [ ] % of the thickness of the nozzle; Then the flaw is transformed into a through-wall axial crack with a length and depth increased by a factor of [ ] times the corresponding values at the time when [ ] depth is reached. Through wall crack growth is then calculated.

   c. Once the through wall crack reaches 2c= [ ] the single edge notched plate solution is utilized for the remainder of the analysis.

   d. SCC crack growth rates are calculated using equation (4) of ASME Code Case N-694-1[5] (developed in MRP-55, Reference [6]), and the stress intensity factors are calculated as above. ASME Code Case N-694-1 is noted as being conditionally acceptable in Regulatory Guide 1.147 Reference [7], subject to the following conditions:

      1. The maximum instantaneous through-thickness stress distribution along the crack front and in the crack-length path must be used to calculate the crack driving force.

2. The stress intensity factor expression of Raju and Newman is only applicable to cylindrical products having a ratio of wall thickness to inside radius between 0.1 and 0.25.

Condition 1 is satisfied since the maximum stress distributions are used to calculate K_I. Condition 2 is not applicable since the Raju Newman solution provided in the code case is not used here.
Equation (4) of ASME Code Case N-694-1 is as follows, when K_I is greater than K_{th} :

$$\dot{a} = \exp\left[-\frac{Q_g}{R}\left(\frac{1}{T}-\frac{1}{T_{ref}}\right)\right]\alpha(K_I - K_{th})^{\beta}$$

where

$\dot{a}$ = crack growth rate at temperature T in m/s
Q_g = thermal activation energy for crack growth
= 130kJ/mole
R = universal gas constant
= 8.314 x 10^{-3} kJ/mole K
T = absolute operating temperature at location of crack, K
= [ ]
T_{ref} = absolute reference temperature used to normalize data
= 598.15K
α = crack growth rate coefficient
= 2.67 x 10^{-12} at 325°C for $\dot{a}$ in units of m/s and K_1 in units of MPa $\sqrt{m}$
K_I = crack tip stress intensity factor, MPa $\sqrt{m}$
K_{th} = crack tip stress intensity factor threshold for SCC
= 9 MPa $\sqrt{m}$ = 8.19 ksi$\sqrt{in}$
β = exponent
= 1.16
When K_I is less than or equal to K_{th}, $\dot{a} = 0$.

The resulting crack growth rate is $\dot{a} = 7.0852 \times 10^{-13}\left(K_I - 9\ MPa\sqrt{m}\right)^{1.16} m/s$

e. The fatigue crack growth rate for each transient is calculated using equation (3) from N-694-1, and stress intensity factor ranges are calculated for each transient. Note that in equation (3) from N-694-1, the rise time is fixed to be 30 seconds. Equation (3) of ASME Code Case N-694-1 is as follows:

$$\frac{da}{dN} = CS_R S_{ENV} \Delta K^n$$

The fatigue crack growth behavior of Alloy 600 materials is affected by temperature, R ratio (K_{min}/K_{max}), and environment. Reference fatigue crack growth rates for PWR water environments are given by:

$C = 4.835 \times 10^{-14} + 1.622 \times 10^{-16}\ T - 1.490 \times 10^{-18}\ T^2 + 4.355 \times 10^{-21}\ T^3$

$S_R = \left[1 - 0.82R\right]^{-2.2}$

$S_{ENV} = 1 + A\left[CS_R \Delta K^n\right]^{m-1} T_R^{1-m}$

where:

$A = 4.4 \times 10^{-7}$
$m = 0.33$
$n = 4.1$
T = degrees C
ΔK = range of stress intensity factor MPa $\sqrt{m}$
$R = K_{min}/K_{max}$
T_R = rise time, set at 30 sec
da/dN = m/cycle

f. For each time step, the crack growth due to SCC and due to fatigue from each transient is calculated and the total growth is accumulated.

7. The through wall crack growth will be calculated at each time interval until the crack reaches the bottom end of the remnant nozzle at a crack length of approximately 2c= [ ] in. Note that cracking through the bottom of the nozzle below the weld does not create a loose parts concern since the material is captured in the recess in the head. After the crack tip reaches the bottom of the nozzle, the single edge notched plate crack will then be propagated until plant license expiration.

8. Additionally, a stability check in accordance with C-5410 of ASME Section XI (Reference [8]) to determine the allowable length of the axial flaw. The calculation will conservatively assume that there is only pressure on the ID of the nozzle such that a tensile hoop stress is generated.

[

]

3.0 ASSUMPTIONS

No unverified or unjustified assumptions are used in this calculation.

Assumptions include the following justified simplifications:

1. To bound crack growth rates, the initial bounding flaw is assumed to be centered near the location of maximum weld residual plus normal operating stress. This location is approximately [ ] inches from the end of the nozzle.

2. As discussed in Appendix A, the bounding initial flaw size is justified based on NDE data.

3. The stress intensity factor solutions from API-579-1 are functions of influence coefficients that are given in tabular form for ratios of wall thickness to inner radius, $t_w / R_i \leq 1.0$. For the remnant nozzle this ratio is: t_w/R_i = [ ]. Since the thicker nozzle provides more constraint against crack opening, it is conservative to use influence coefficients calculated for $t_w/R_i = 1.0$ for the present flaw growth evaluations.
4. Growth rates of the through wall crack are greater on the outside wall than at the inside wall. The larger of the two rates is used to calculate through wall crack growth, which overestimates the actual crack growth along the nozzle.
5. Faulted loads (SSE and Loss of Secondary Pressure, LSP) are not applicable to this evaluation since they do not contribute to growth of cracks under PWSCC or fatigue crack growth under cyclic loading conditions.
6. The loads due to OBE, Hydraulic Flow, White Noise, Pump Periodic Excitation and Vortex Shedding result in bending moments and corresponding axial stresses in the nozzle, that are negligibly small, and would not contribute to growth of the existing radial axial flaws in the nozzle due to fatigue or PWSCC.
7. The Hydrostatic test is not included in fatigue evaluations, since the [ ] cycles will result in negligible crack growth in comparison to PWSCC crack growth. Also, excluding the immediate vicinity of the J-Groove weld the hoop stress along the nozzle length due to a hydrostatic test is a compressive hoop stress equal in magnitude to the applied pressure, which results in $\sigma_m + p_c \approx 0$ (i.e., no driving force for crack growth).

4.0 ANALYSIS INPUTS

4.1 Geometry and Material

Dimensions used in the flaw growth analysis are:

Outside Diameter of BMI Nozzle: [ ] inches, Reference [9].

Inside diameter of BMI Nozzle: [ ] inches, Reference [9].

The remnant BMI Nozzle is ASME SB-166, Alloy 600 material, Reference [12].

4.2 Bounding Initial Flaw Size

See Appendix A.

4.3 Loading Data and Stresses

Applicable design transients, cycles and external loads are specified in References [10] and [11].

Condition	Transient	Filename Convention	Number of Cycles	Figure in Reference [11]
Normal	Heatup, [ ]	HUup/HUlow	[ ]	Fig. 2
	Cooldown, [ ]	CDup/CDlow	[ ]	Fig. 2
	Plant Loading, 5% min.	PL	[ ]	Fig. 3
	Plant Unloading, 5% min.	PU	[ ]	Fig. 3
	10% Step Load Increase	NVAR	[ ]	[ ] [ ]
	10% Step Load Decrease			
	Normal Plant Variation			
Upset	Reactor Trip Loss of Reactor Coolant Flow Loss of Load	RT	[ ]	Fig. 4
	OBE	-	[ ]	-
Faulted	Loss of Secondary Pressure	LSP	[ ]	Fig. 5
Test	Hydrostatic Test, [ ] °F – [ ] °F	-	[ ]	-
	Leak Test, [ ] psia, [ ] °F – [ ] °F	LEAK	[ ]	-

Other external loads include [11]:

- Hydraulic Flow
- Seismic (SSE)
- White Noise
- Pump Periodic Excitation
- Vortex Shedding

The normal operating inlet water temperature is [ ] [11].

The operating pressure is [ ] [12].

Weld residual stresses, normal operating stresses and stresses for all design transients and due to all external loads are taken from References [3] and [4].

5.0 CALCULATIONS

Detailed calculations are contained in Mathcad and Excel files attached with this calculation (See Appendix B).

5.1 Path Lines for Stresses

Stresses for the crack growth analysis were evaluated on the path lines shown in Figure 5-1.

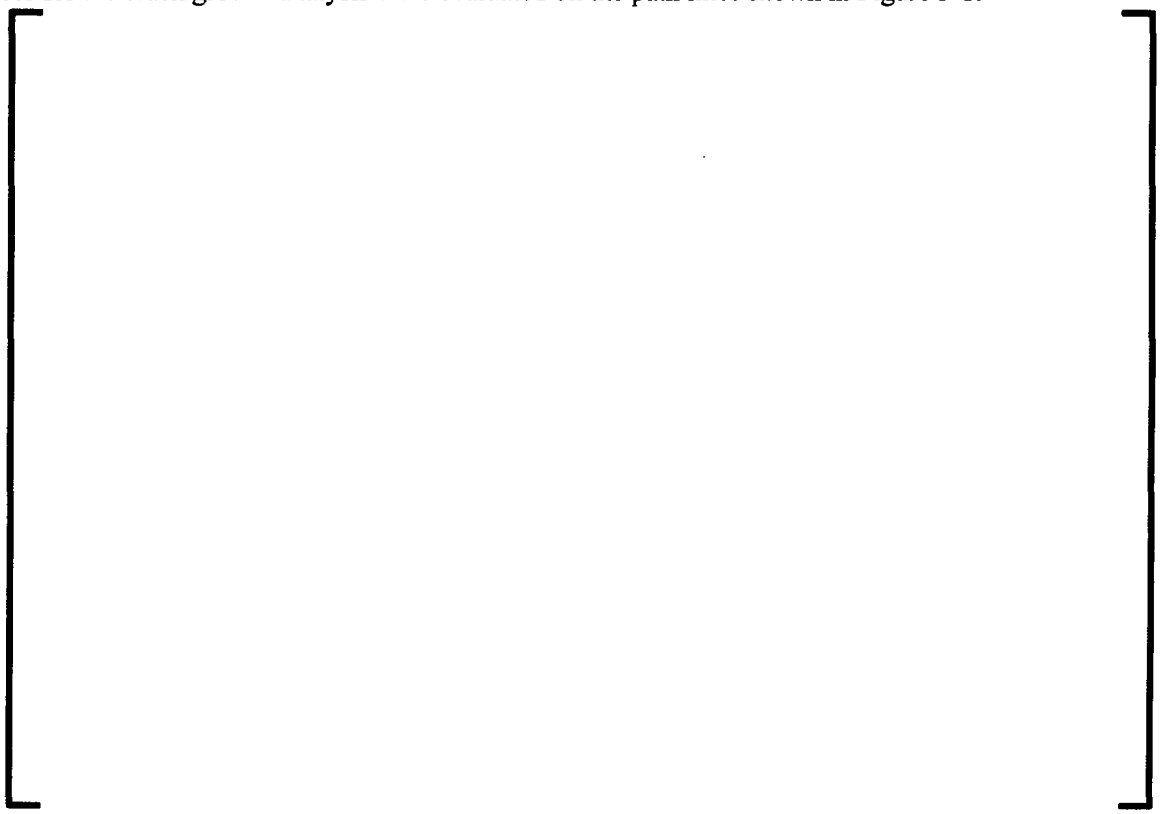

Figure 5-1: Path Lines for Stresses

5.2 Growth of Initial Surface Crack

Details of the calculation of crack growth for the longitudinal surface flaw are contained in the Mathcad files named *"Surface_crack_growth.xmcd", "Polynomial.xmcd", "API_Table13.xmcd","Interpolate3d.xmcd", "KCSCLE2.xmcd", "Influence_coeff_outside_surface_crack.xmcd", and "Fatigue_Crack_Growth.xmcd".*

Surface crack growth is calculated using hoop stresses from the pathline labeled P12 in Figure 5-1. Weld residual stresses and weld residual plus operating stresses are input to Mathcad using the files "*WRS_Path12.csv*" and "*WRS_OP_Path12.csv*". Transient stresses as input to matrices using the Mathcad file "*Transients_P12.xmcd.*

A summary of results from the calculation of crack growth for the longitudinal surface flaw is given in Table 5-1.

At approximately [ ] months or [ ] years, the crack depth, a, will grow to [ ] of the wall thickness. At that time, the crack length, $2c$ is approximately [ ] inches. The flaw is then assumed to be transformed into a though-wall axial crack with a length and depth increased by a factor of [ ] times

the corresponding values at the time when [ ] depth is reached. Thus the initial length for through wall crack growth is $2c$ = [ ] x [ ] = [ ] inches.

Table 5-1: Crack Growth Calculation for Longitudinal Surface Flaw

Time, t (month)	Growth of crack depth,a					Growth of crack length, 2c				2c/a
			SCC		FCG		SCC		FCG	
	a (in)	a/t_w	K_I (ksi*in^0.5)	da/dt (in/yr)	da/dt (in/yr)	2c (in)	K_I (ksi*in^0.5)	dc/dt (in/yr)	dc/dt (in/yr)	
[ ]										

5.3 Growth of Through Wall Crack

Details of the calculation of crack growth for the longitudinal surface flaw are contained in the Mathcad files named *"Through_crack_growth-BC.xmcd", "API_Table_6_and_7.xmcd", and "Fatigue_Crack_Growth.xmcd".*

Weld residual stresses and weld residual plus operating stress as a function of crack length are calculated in the Mathcad files "*WRS_MB.xmcd*", and "*WRS_OP_MB.xmcd*". Transient stresses as a function of crack length are calculated in Mathcad files "*Transients_MB.xmcd*. The trapezoidal rule was used to average hoop membrane and bending stress over the length of the through wall crack.

A summary of results from the calculation of crack growth for the longitudinal through wall flaw is given in Table 5-2. The results show that in [ ] months or [ ] years, the crack length will grow to 2c= [ ] at which time the crack tip will be located near the bottom end of the remnant nozzle.

Table 5-2: Crack Growth Calculation for Longitudinal Through Wall Flaw

Time, t (month)	2c (in)	SCC					FCG
		σ_m (ksi)	σ_b (ksi)	K_I at inside wall (ksi*in^0.5)	K_I at outside wall (ksi*in^0.5)	dc/dt (in/yr)	dc/dt (in/yr)
[							]

Time, t (month)	2c (in)	SCC					FCG
		σ_m (ksi)	σ_b (ksi)	K_I at inside wall (ksi*in^0.5)	K_I at outside wall (ksi*in^0.5)	dc/dt (in/yr)	dc/dt (in/yr)

Time, t (month)	2c (in)	SCC					FCG
		σ_m (ksi)	σ_b (ksi)	K_I at inside wall (ksi*in^0.5)	K_I at outside wall (ksi*in^0.5)	dc/dt (in/yr)	dc/dt (in/yr)

Time, t (month)	2c (in)	SCC					FCG
		σ_m (ksi)	σ_b (ksi)	K_I at inside wall (ksi*in^0.5)	K_I at outside wall (ksi*in^0.5)	dc/dt (in/yr)	dc/dt (in/yr)

5.4 Growth of Single Edge Notched Plate Crack

Once the crack reaches the bottom of the nozzle (2c= [ ]) the crack growth is calculated based on a single edge cracked plate stress intensity factor solution. Since the results of the previous section indicate that fatigue crack growth is small compared to PWSCC, fatigue crack growth is not evaluated. The welding residual stress (WRS) plus operating stress results are supplied up to path P23 in Reference [3]. Review of the results indicates that by path P23 the residual stresses have decayed and thus the stresses will be constant and equal to those at path P23 above that point.

Based on the dimensions from the references noted the length of the remnant nozzle is calculated to be [ ] as shown below.

Height from RVBH CL to bottom of nozzle	=	[ ]	(Reference [9])
Radial distance from vessel CL to nozzle OD	=	[ ]	(Reference [13])
RVBH outside radius	=	[ ]	(Reference [14])
Height from RVBH CL to RVBH OD at nozzle OD	=	[ ]	
Length of nozzle below vessel	=	[ ]	
Length of nozzle removed in RVBH bore	=	[ ]	(Reference [9]), Step 5
Length of nozzle removed	=	[ ]	
Length of original nozzle	=	[ ]	(Reference [9])
Length of remnant nozzle	=	[ ]	

The stress intensity solution for the single edge notched plate uses a plate width of 2b = [ ].

At the time the crack growth to the bottom of the nozzle a total of [ ] months have elapsed. To reach plant license expiration in 2047 the single edge notched plate crack growth is calculated for an additional [ ] months ([ ] years) in Table 5-3. After [ ] months the crack grows to a= [ ], which results in a remaining un-cracked ligament of approximately [ ] inches at the top of the remnant nozzle. The calculation is performed in the spreadsheet *"Nozzle_CG.xlsm"*. An example of the calculation of K_I performed in the spreadsheet is shown below for the first time step.

[ ]

Table 5-3: Crack Growth Calculation for Single Edge Notched Plate

Month	a (in)	σ_m (ksi)	σ_b (ksi)	K_I (MPa$\sqrt{m}$)	$\dot{a}$ (in/year)	da (in)
[						]

Month	a (in)	σ_m (ksi)	σ_b (ksi)	K_I (MPa$\sqrt{m}$)	$\dot{a}$ (in/year)	da (in)

Month	a (in)	σ_m (ksi)	σ_b (ksi)	K_I (MPa$\sqrt{m}$)	$\dot{a}$ (in/year)	da (in)

Month	a (in)	σ_m (ksi)	σ_b (ksi)	K_I (MPa$\sqrt{m}$)	$\dot{a}$ (in/year)	da (in)

Month	a (in)	σ_m (ksi)	σ_b (ksi)	K_I (MPa$\sqrt{m}$)	$\dot{a}$ (in/year)	da (in)

Month	a (in)	σ_m (ksi)	σ_b (ksi)	K_I (MPa$\sqrt{m}$)	$\dot{a}$ (in/year)	da (in)

5.5 Stability Check

Per article C-5410 of Reference [8], the allowable length of an axial flaw is given by

$$l_{allow} = 1.58(R_m t)^{0.5}\left[\left(\frac{\sigma_f}{\sigma_h}\right)^2 - 1\right]^{0.5}$$

where:

$\sigma_f = flow\ stress = \frac{1}{2}(S_y + S_u) = \frac{1}{2}(27.9\ ksi + 80\ ksi) = 53.95\ ksi$, Alloy 600 at 600°F (Reference [15])

$R_m = Mean\ radius =$ [ ]

$t = wall\ thickness =$ [ ]

$\sigma_h = \frac{pR_m}{t} =$ [ ]

Inserting the values above results in

$l_{allow} =$ [ ]

Since the nozzle tapers over the length the calculation is also performed based on the dimensions of the thinnest section (OD = [ ], ID = [ ], Reference [16]).

$R_m = Mean\ radius =$ [ ]

$t = wall\ thickness =$ [ ]

$\sigma_h = \frac{pR_m}{t} =$ [ ]

Inserting the values above results in

$l_{allow} =$ [ ]

The final allowable length is then calculated using a weighted average of the thin section and the thick section considering the thin section to be [ ] (DIM "B", Reference [16], rounded up) and the thick section to make up the remainder.

$l_{allow} =$ [ ]

Since l_{allow} = [ ] is greater than the final flaw size of [ ] this criterion is satisfied.

6.0 SUMMARY OF RESULTS

Based on NDE, an initial surface crack with depth, a= [ ], and length, 2c= [ ] was postulated. This crack will grow to be through wall in [ ] years at which time it will have a length, 2c= [ ].

In an additional [ ] years, the crack length will grow to 2c= [ ], at which time it will grow through the bottom portion of the nozzle.

In the remaining [ ] years until plant license expiration in 2047 the crack grows up the nozzle to a total length of approximately a= [ ]. This leaves a remaining un-cracked ligament of approximately [ ] inches at the top of the nozzle so the generation of loose parts is unlikely.

Figure 6-1 shows a sketch of the progression of the crack growth.

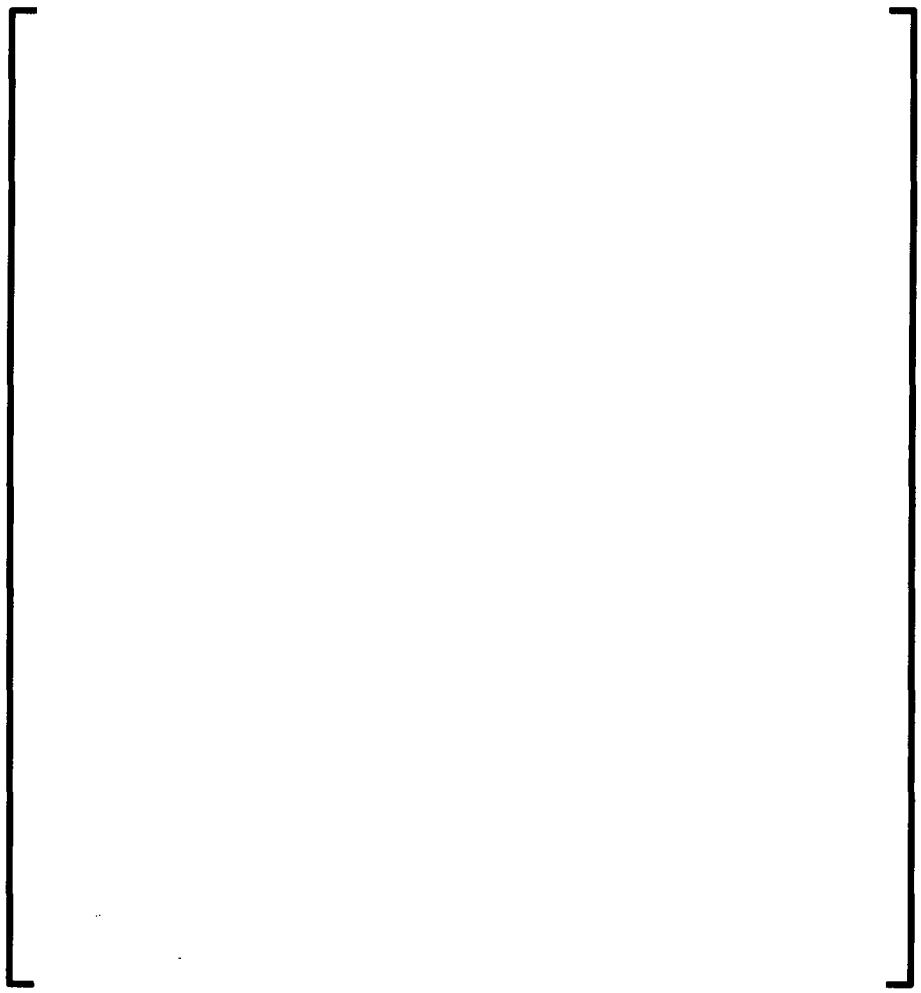

Figure 6-1: Sketch of Flaw Growth Progression

7.0 REFERENCES

References identified with an (*) are maintained within the Palo Verde Records System and are not retrievable from AREVA Records Management. These are acceptable references per AREVA Administrative Procedure 0402-01, Attachment 8. See page [2] for Project Manager Approval of customer references.

1. API 579-1/ASME FFS-1 2007, "Fitness-For-Service", Second Edition, June 5, 2007.
2. S.T. Rolfe and J.M. Barsom, "Fracture and Fatigue Control in Structures – Applications of Fracture Mechanics", Prentice-Hall, Englewood Cliffs, New Jersey, 1977
3. AREVA Document Number 32-9215089-001, "Weld Residual Stress Analysis for PVNGS3 RV BMI Nozzle Repair," Proprietary.
4. AREVA Document Number 32-9215084-001, "ASME Section III End of Life Analysis of PVNGS3 RV BMI Nozzle Repair," Proprietary.
5. ASME Code Case N-694-1 "Evaluation Procedure and Acceptance Criteria for PWR Reactor Vessel Head Penetration Nozzles," Section XI, Divisions 1, Approved February 20, 2004.
6. *Materials Reliability Program (MRP) Crack Growth Rates for Evaluating Primary Water Stress Corrosion Cracking (PWSCC) of Thick-Wall Alloy 600 Materials (MRP-55) Revision 1*, EPRI, Palo Alto, CA: 2002. 1006695.
7. Regulatory Guide 1.147, Revision 16, "Inservice Inspection Code Case Acceptability, ASME Section XI, Division 1", October 2010.
8. ASME Boiler and Pressure Vessel Code, Section XI, "Rules for Inservice Inspection of Nuclear Power Plant Components", 2001 Edition including Addenda through 2003.
9. AREVA Drawing 02-9212754E-001, "Palo Verde Unit 3, Bottom Mounted Instrument Nozzle Repair (Penetration 3)".
10. *Report N001-0301-00214, Revision 7, "Reactor Vessel, Unit 3, Analytical Report, V-CE-30869, 30AU84.
11. *Specification N001-0301-00006, Revision 6, "General Specification for Reactor Vessel Assembly."
12. AREVA Document Number 08-9212780-001,"Palo Verde Unit 3 Reactor Vessel Bottom Mounted Instrument Nozzle Modification," Proprietary.
13. *PVNGS Document N001-0301-00530, Revision 0, "Bottom Head Penetrations – Arizona Public Service III, 182.25 ID PWR".
14. *PVNGS Document N001-0301-00054, Revision 2, "General Arrangement Arizona Public Service III 182.25 ID Reactor Vessel".
15. ASME Boiler and Pressure Vessel Code, Section III, "Nuclear Power Plant Components", Division 1, 1971 Edition including Addenda through Winter 1973.
16. *PVNGS Document N001-0603-00208, Revision 3, "Bottom Head Instrument Tubes".

APPENDIX A: BOUNDING AXIAL FLAW IN NOZZLE

A.1 Purpose

Non-destructive examination (NDE) of the Palo Verde Unit 3 bottom mounted instrumentation (BMI) nozzle #3 by ultrasonic inspection (UT) revealed ten flaw indications in the nozzle in the vicinity of the partial penetration J-groove weld that attaches the nozzle to the reactor vessel bottom head. The purpose of this appendix is to define a bounding axial flaw for use in a flaw growth analysis that examines the potential for the flaw to grow to the ends of the nozzle during the remaining life of the plant and possibly create a loose part.

A.2 Definition of Flaw Indications and Calculation of Nozzle Cutout

The NDE inspection report [1] describes ten part-through wall flaw indications in BMI nozzle #3 located on the outside surface of the nozzle near the J-groove weld. Flaw indications 1 through 4 are oriented primarily in the axial direction (with respect to the nozzle) while flaw indications 5 through 10 are slightly skewed. It is postulated that over time the "axial" flaws (indications 1 through 4) and the skewed flaws (indications 5 through 10) will increase in depth and length until they link up, at which time the skewed flaws will be considered to have arrested. It is further postulated that the axial flaws will continue to grow along the length of the nozzle until they either arrest or reach the ends of the nozzle. [

]

Table A-1 and Table A-2 are taken from the UT inspection report [1]. Table A-1 presents the inspection data for flaw indications 1 through 4 and Table A-2 provides similar data for flaw indications 5 through 10. Each flaw indication is defined by linear (L1/L2) and angular (ϕ1/ϕ2) positions of its two end points, relative to horizontal and vertical datum lines. The vertical position of the weld at the location of the flaw indication is defined by the linear dimensions L3 and L4. The reference positions for these parameters are explained below, with the aid of Figure A-1.

Distance is measured in inches.
Angular position is measured in degrees.

Horizontal datum: [ ]

Azimuthal datum: [ ]
[ ]

The UT data in Table A-1 and Table A-2 are rearranged and processed in Table A-3 to determine bounding flaw characteristics. The bounding axial flaw is defined to be [ ] deep and [ ] long, extending from [ ] to [ ] below the horizontal datum.

A.3 References

1. *Palo Verde Unit 3 U3R17, Reactor Vessel Bottom Mounted Instrumentation ID Examinations, Wesdyne Report WDI-PJF-1312161-FSR-001, Rev. 0, October 2013.

Figure A-1: Reference Positions for UT Inspection Data

Table A-1: UT Data for Flaw Indications 1 Through 4

[

]

Table A-2: UT Data for Flaw Indications 5 Through 10

[

]

Table A-3: Calculation of Nozzle Cutout

[

]

APPENDIX B: COMPUTER FILES

Computer files used in this analysis have been stored in the ColdStor directory :

"\cold\General-Access\32\32-9000000\32-9217241-000\official"

All files, listed in Table B-1, were uploaded to ColdStor on 24 Feb 2014.

Computer files used in revision 001 of this analysis are stored in the ColdStor directory:

"\cold\General-Access\32\32-9000000\32-9217241-001\official"

The revision 001 computer files are listed in Table B-2. The following files from revision 000 (Table B-1) are superseded by the indicated files from revision 001 (Table B-2):

Rev. 000 File (Table B-1)	**Rev. 001 File (Table B-2)**
API_Table_6_and_7.xmcd	API_Table_6_and_7.xmcd
Through_crack_growth.xmcd	Through_crack_growth-BC.xmcd
ThroughCrackGrowth_SCC_FCG.txt	ThroughCrackGrowth_SCC_FCG.txt

Table B-1: List of Revision 000 Computer Files

CheckSum	Permissions	User	Size	Month	Day	Year	Time	Filename
\cold\General-Access\32\32-9000000\32-9217241-000\official								
0	drwxdc	Masnyder	0	Feb	17	2014	9:46:08	Fatigue_Crack_Growth
0	drwxdc	Masnyder	0	Feb	21	2014	13:37:02	Outside_Surface_Crack_SIF
0	drwxdc	Masnyder	0	Feb	21	2014	13:44:06	Through_Wall_Crack_SIF
0	drwxdc	Masnyder	0	Feb	21	2014	14:37:46	Transient_stresses
0	drwxdc	Masnyder	0	Jan	30	2014	9:25:51	WRS_OP_stresses
./Fatigue_Crack_Growth:								
32173	-rw-dc	Masnyder	75405	Feb	17	2014	9:46:08	Fatigue_Crack_Growth.xmcd:1
./Outside_Surface_Crack_SIF:								
26967	-rw-dc	Masnyder	354816	Jan	20	2014	14:04:23	API_579-1_Tables.xls:1
49679	-rw-dc	Masnyder	906247	Jan	19	2014	22:34:28	API_Table13.xmcd:1
21094	-rw-dc	Masnyder	23792	Feb	21	2014	13:36:59	CrackGrowth_SCC_FCG.txt:1
46601	-rw-dc	Masnyder	265511	Jan	19	2014	22:35:17	Influence_coeff_outside_surface_crack.xmcd:1
13138	-rw-dc	Masnyder	156663	Feb	17	2014	11:22:36	Interpolate3d.xmcd:1
53723	-rw-dc	Masnyder	46293	Jan	19	2014	22:37:52	KCSCLE2.xmcd:1
16789	-rw-dc	masnyder	34224	Jan	19	2014	10:04:43	Polynomial.xmcd:1
56179	-rw-dc	masnyder	2793267	Feb	21	2014	13:36:45	Surface_crack_growth.xmcd:1
30509	-rw-dc	masnyder	1797	Jan	22	2014	15:26:31	WRS_OP_Path12.csv:1
32071	-rw-dc	masnyder	18144	Jan	22	2014	15:26:13	WRS_OP_Path12.xlsx:1
40680	-rw-dc	masnyder	1780	Jan	25	2014	19:41:47	WRS_Path12.csv:1
23961	-rw-dc	masnyder	13619	Jan	25	2014	19:41:13	WRS_Path12.xlsx:1
3047	-rw-dc	masnyder	53811	Jan	18	2014	18:37:36	c_13.csv:1
./Through_Wall_Crack_SIF:								
43129	-rw-dc	masnyder	401399	Feb	17	2014	12:27:19	API_Table_6_and_7.xmcd:1
31505	-rw-dc	masnyder	122484	Feb	21	2014	13:38:06	ThroughCrackGrowth_SCC_FCG.txt:1
50605	-rw-dc	masnyder	3132947	Feb	21	2014	13:44:02	Through_crack_growth.xmcd:1
62564	-rw-dc	masnyder	1541	Jan	20	2014	14:04:52	c_6.csv:1

CheckSum	Permissions	User	Size	Month	Day	Year	Time	Filename
12859	-rw-dc	masnyder	1557	Jan	20	2014	14:05:51	c_7.csv:1
./Transient_stresses:								
60992	-rw-dc	masnyder	32670	Jan	23	2014	17:55:04	CDlow_mb_sum.dat:1
62349	-rw-dc	masnyder	68763	Jan	23	2014	17:55:04	CDlow_path_12.dat:1
9602	-rw-dc	masnyder	32670	Jan	24	2014	7:45:08	CDup_mb_sum.dat:1
58779	-rw-dc	masnyder	68763	Jan	24	2014	7:45:08	CDup_path_12.dat:1
27397	-rw-dc	masnyder	32670	Jan	23	2014	17:38:20	HUlow_mb_sum.dat:1
39873	-rw-dc	masnyder	68763	Jan	23	2014	17:38:20	HUlow_path_12.dat:1
26577	-rw-dc	masnyder	32670	Jan	23	2014	17:29:42	HUup_mb_sum.dat:1
58736	-rw-dc	masnyder	68763	Jan	23	2014	17:29:42	HUup_path_12.dat:1
38729	-rw-dc	masnyder	1815	Jan	23	2014	18:28:56	LEAK_mb_sum.dat:1
40359	-rw-dc	masnyder	3942	Jan	23	2014	18:28:56	LEAK_path_12.dat:1
4531	-rw-dc	masnyder	59895	Jan	23	2014	18:28:06	LSP_mb_sum.dat:1
17201	-rw-dc	masnyder	125958	Jan	23	2014	18:28:06	LSP_path_12.dat:1
62683	-rw-dc	masnyder	19965	Feb	18	2014	11:40:21	NVAR_mb_sum.dat:1
3076	-rw-dc	masnyder	42072	Feb	18	2014	11:40:21	NVAR_path_12.dat:1
17058	-rw-dc	masnyder	2509	Jan	24	2014	14:37:50	P12_x_t.csv:1
52454	-rw-dc	masnyder	21780	Jan	23	2014	18:00:44	PL_mb_sum.dat:1
8543	-rw-dc	masnyder	45885	Jan	23	2014	18:00:44	PL_path_12.dat:1
50182	-rw-dc	masnyder	19965	Jan	23	2014	18:05:58	PU_mb_sum.dat:1
43941	-rw-dc	masnyder	42072	Jan	23	2014	18:05:58	PU_path_12.dat:1
45487	-rw-dc	masnyder	25410	Jan	23	2014	18:12:36	RT_mb_sum.dat:1
31684	-rw-dc	masnyder	53511	Jan	23	2014	18:12:36	RT_path_12.dat:1
65034	-rw-dc	masnyder	292	Feb	21	2014	10:58:52	Transient_events.csv:1
31021	-rw-dc	masnyder	24285	Feb	20	2014	15:47:42	Transients_Bending.csv:1
50929	-rw-dc	masnyder	324817	Feb	21	2014	10:59:48	Transients_MB.xlsm:1
10696	-rw-dc	masnyder	1434290	Feb	21	2014	11:01:20	Transients_MB.xmcd:1
3137	-rw-dc	masnyder	27655	Feb	20	2014	15:47:06	Transients_Membrane.csv:1
37330	-rw-dc	masnyder	103608	Feb	20	2014	14:15:49	Transients_P12.csv:1

CheckSum	Permissions	User	Size	Month	Day	Year	Time	Filename
30899	-rw-dc	masnyder	613391	Feb	21	2014	10:58:32	Transients_P12.xlsm:1
1553	-rw-dc	masnyder	703975	Feb	21	2014	11:00:30	Transients_P12.xmcd:1
./WRS_OP_stresses:								
0	drwxdc	masnyder	0	Jan	30	2014	9:24:32	FracturePP_Nozzle_Loads
64441	-rw-dc	masnyder	265411	Jan	28	2014	21:43:36	WRS_MB.xmcd:1
11001	-rw-dc	masnyder	272075	Jan	28	2014	21:43:28	WRS_OP_MB.xmcd:1
35403	-rw-dc	masnyder	1779	Jan	21	2014	11:40:21	WRS_OP_mb_sum.dat:1
16740	-rw-dc	masnyder	1156517	Jan	21	2014	11:46:44	WRS_OP_path_results.pdf:1
54429	-rw-dc	masnyder	87023	Jan	21	2014	11:40:21	WRS_OP_paths.dat:1
33323	-rw-dc	masnyder	1779	Jan	21	2014	11:40:39	WRS_mb_sum.dat:1
23762	-rw-dc	masnyder	1148814	Jan	21	2014	11:48:02	WRS_path_results.pdf:1
52190	-rw-dc	masnyder	87023	Jan	21	2014	11:40:39	WRS_paths.dat:1
./WRS_OP_stresses/FracturePP_Nozzle_Loads:								
47281	-rw-dc	masnyder	3668	Jan	29	2014	12:26:28	RemNoz_HF_mb_sum.dat:1
26278	-rw-dc	masnyder	7793	Jan	29	2014	12:26:28	RemNoz_HF_path_12.dat:1
49126	-rw-dc	masnyder	3668	Jan	29	2014	12:29:58	RemNoz_OBE_mb_sum.dat:1
43572	-rw-dc	masnyder	7793	Jan	29	2014	12:29:58	RemNoz_OBE_path_12.dat:1
62457	-rw-dc	masnyder	3668	Jan	29	2014	12:28:42	RemNoz_PPE_mb_sum.dat:1
11288	-rw-dc	masnyder	7793	Jan	29	2014	12:28:42	RemNoz_PPE_path_12.dat:1
7071	-rw-dc	masnyder	3668	Jan	29	2014	12:31:14	RemNoz_SSE_mb_sum.dat:1
8843	-rw-dc	masnyder	7793	Jan	29	2014	12:31:14	RemNoz_SSE_path_12.dat:1
9840	-rw-dc	masnyder	3668	Jan	29	2014	12:32:26	RemNoz_WN_mb_sum.dat:1
26387	-rw-dc	masnyder	7793	Jan	29	2014	12:32:26	RemNoz_WN_path_12.dat:1

Table B-2: List of Revision 001 Computer Files

CheckSum	Permissions	User	Size	Month	Day	Year	Time	Filename
\cold\General-Access\32\32-9000000\32-9217241-001\official								
0	drwxdc	triordan	0	Mar	24	2014	9:48:06	SENP_Crack
0	drwxdc	triordan	0	Mar	24	2014	9:47:10	Through_Wall_Crack_SIF
./SENP_Crack:								
49914	-rw-dc	triordan	286588	Mar	27	2014	8:38:45	Nozzle_CG.xlsm
./Through_Wall_Crack_SIF:								
48879	-rw-dc	triordan	401905	Mar	20	2014	16:20:39	API_Table_6_and_7.xmcd
53027	-rw-dc	triordan	120971	Mar	23	2014	15:14:58	ThroughCrackGrowth_SCC_FCG.txt
47255	-rw-dc	triordan	3115328	Mar	23	2014	15:28:40	Through_crack_growth-BC.xmcd

Enclosure
Relief Request 52 Proposed Alternative in Accordance with
10 CFR 50.55a(a)(3)(i)

ATTACHMENT 6

Natural Frequency and Structural Integrity Analysis Natural Frequency and Structural Integrity Analysis for PVNGS Unit 3 RV BMI Nozzle Repair